2017-01-2135

A Fuel Cell System Sizing Tool based on Current Production Aircraft

Author, co-author (Do NOT enter this information. It will be pulled from participant tab in MyTechZone)

Affiliation (Do NOT enter this information. It will be pulled from participant tab in MyTechZone)

Abstract

Electrification of aircraft is on track to be a future key design principal due to the increasing pressure on the aviation industry to significantly reduce harmful emissions by 2050 and the increased use of electrical equipment. This has led to an increased focus on the research and development of alternative power sources for aircraft, including fuel cells. These alternative power sources could either be used to provide propulsive power or as an Auxiliary Power Unit (APU). Previous studies have considered isolated design cases where a fuel cell system was tailored for their specific application. To accommodate for the large variation between aircraft, this study covers the design of an empirical model, which will be used to size a fuel cell system for any given aircraft based on basic design parameters. The model was constructed utilising aircraft categorisation, fuel cell sizing and balance of plant sub-models. Fifteen aircraft categories were defined based on the primary function and propulsion method of the aircraft. For each category, propulsive power and electrical generation requirements were calculated. Based on the results from categorisation and the flight envelope of the aircraft, fuel cell and balance of plant systems are defined. The total system mass and volume are given as outputs, along with polarisation and power curves for the fuel cell. This study finds that the model can accurately predict the electrical generation capability and propulsive requirements across the defined aircraft categories. In addition, the model can appropriately define key, high-level fuel cell parameters based on current Polymer Electrolyte Membrane (PEM) technology. Total fuel cell system mass and volume are calculated and shown to be reasonable for small aircraft. For larger aircraft with a Maximum Take-Off Weight (MTOW) greater than 50,000kg, current PEM technology is not able to match the gravimetric power density of existing APUs.

Introduction

Electrification of aircraft is on track to be a key design principal in the future due to the increasing pressure on the whole aviation industry to significantly reduce harmful emissions by 2050 [1]. This has led to an increased focus on the research and development of alternative power sources for aircraft, including fuel cells. These alternative power sources could either be used to provide propulsive power or as an Auxiliary Power Unit (APU).

Hydrogen fuel cells produce electricity through an exothermic electrochemical reaction between hydrogen and oxygen. This highly efficient reaction only produces heat and water as by-products [2]. Two Fuel Cell (FC) technologies currently being researched for use in aerospace applications are Solid Oxide Fuel Cells (SOFC) and Polymer Electrolyte Membrane (PEM) fuel cells. A key difference between these two technologies is their operating temperature. The significantly higher operating temperature of a SOFC (700-1,000°C) compared with 60-100°C for a PEM FC [3] allows it to reform light fossil fuels such as methane into hydrogen. However, if PEM fuel cells are used, then their relatively low operating temperature could potentially reduce the thermal signature of the electrical generation and/or propulsive system of the aircraft.

Several studies have previously considered the integration of fuel cell systems into aircraft [4-18]. Different aspects of the integration process have been considered. These included the theoretical integration of a FC system to partially cover the electrical load on the APU on a Boeing 787-8 [14]. In addition, working prototypes on a small remote piloted scale have been designed and flown [4-6, 9-11]. The success of these studies has ranged from flights of three minutes to over two hours on FC power.

Each previous study looked at their aircraft as an isolated design case and tailored the FC system for their specific application. As there are a large range of airframe types, each suited to a particular mission profile, there will be a wide range of performance requirements placed on the FC system. To accommodate this large variation, this paper will cover the design of an empirical model, which will be designed to size a PEM FC system for any given aircraft based on basic design parameters.

This paper aims to develop a method of predicting aircraft electrical generation capability and propulsive requirements. A model to size a PEM FC system for any aircraft as either a propulsive power provider or APU will also be developed. This will be designed as a guide for aircraft Original Equipment Manufacturers (OEM).

Methodology

Empirical modelling work was split into three main sections: aircraft categorisation, fuel cell modelling and balance of plant calculations. These were then combined to make the full model.

Aircraft Categorisation

Data for 527 aircraft were collected for categorisation [19-29]. Aircraft were categorised using a two-step method. Initially, 11 categories were defined based on an aircraft's primary role and easily distinguishable physical characteristics. These categories are summarised in Table 1. Each category was further subdivided based on its propulsion method into those propelled by a propeller and those propelled by a jet derived engine. This gave a total of 15 sub-categories for the model to be based on.

Table 1. Aircraft category definitions

Aircraft category	Key characteristics
Fuel cell	Primary power source must be a Fuel Cell (FC). The aircraft can be either manned or unmanned.
All electric	Propulsion must be provided by an electric motor and electricity must not be supplied by a fuel cell.
Unmanned	Any fixed wing aircraft which is either remotely piloted or autonomously controlled and is neither 'all electric' or powered by a fuel cell.
Bomber and surveillance	Aircraft designed for the primary role of dropping ordinance or performing surveillance.
Fighter and trainer	A manned aircraft with a primary role as a military fighter or trainer. These aircraft typically have a high thrust to weight ratio.
Transport	Typically, a military aircraft for transporting personnel. Aircraft in this category generally have Maximum Take-Off Weight (MTOW) greater than 100,000kg.
Airliner and freighter	Typically, large multiengine aircraft.
Business	An aircraft typically designed for transporting small groups of people. This category also includes privatised versions of larger aircraft.
Utility	Typically, a small general-purpose aircraft for transporting people or freight.
Amphibian	More specialised aircraft designed to take-off from and land on water.
Lightplane	Any aircraft that does not fit into another category and has a MTOW less than 3500kg.

For each sub-category, the Maximum Take-Off Weight (MTOW) was related to either the propulsive power or maximum thrust produced by the aircraft. This provided a good correlation as expected from the form of the standard aircraft power and thrust equations which directly relate the power or thrust required to aircraft weight [30].

Changes in MTOW were also found to correlate well with the electrical generation capability of each of the aircraft. The electrical generation capability of an aircraft was defined as the total capacity of all engine mounted generators as well as any capability provided by an APU.

Each relationship was refined systematically by curve fitting the model results with the raw aircraft data using the least squares method. When considering trendline options in Excel, the focus was on linear and polynomial types as exponential and power lines lead to an inaccurate coefficient of determination (R^2) [31]. When considering the regression analysis carried out by Excel, R^2 can have a value between zero and one. The larger the value of R^2 the smaller the residual sum of squares and therefore the better fit the trendline is to the data [32].

Figure 1 shows an example of the refined relationships for existing FC powered aircraft. All the aircraft used in the construction of this chart were propelled by a propeller attached to an electric motor.

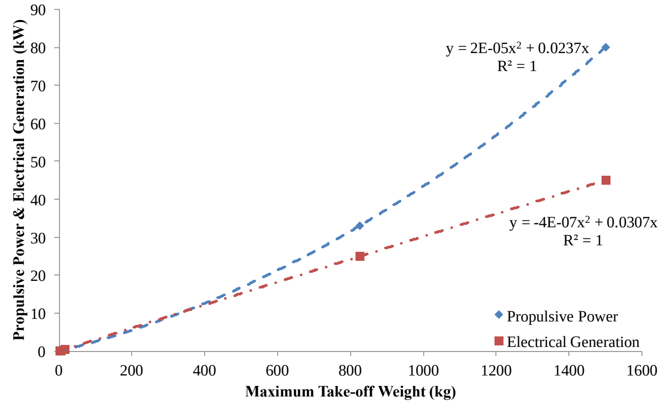

Figure 1. Refined correlations for existing fuel cell powered aircraft

Fuel Cell Sizing Model

A simplified FC model was used to find the fuel and oxidant requirements as well as an estimated mass and volume for the stack. Fuel, in this case hydrogen (H_2) usage was found using Equation 1 [33]. Scaling factors, shown in Table 2 were used to set the FC power (P_{elec}) higher than the output from the aircraft model. This was done to allow for degradation of the FC over time as well as increased flexibility for peak loads.

$$\dot{m}_{H_2} = \frac{M_{H_2} P_{elec} \lambda}{2 V_c F} \quad (1)$$

Where,
$\dot{m}_{H_2}$ = hydrogen mass flow rate required by the stack (kg/s)
M_{H_2} = molar mass of hydrogen (2.016g/mol [34])
P_{elec} = fuel cell electrical power request (W)
λ = stoichiometric ratio
V_c = average cell voltage (V)
F = Faraday constant (96,485C/mol [30])

Table 2. Fuel cell power scaling factors

Fuel cell purpose	Scaling factor
Propulsive power	$P_{elec} = 1.5 P_{aircraft\ model}$
APU	$P_{elec} = 1.2 P_{aircraft\ model}$

Fuel cells can either be of an air breathing or air independent design. Oxidant usage, in the form Oxygen (O_2) either from air or from on-board O_2 storage was calculated using Equation 2 [33].

$$\dot{m}_{O_2} = \frac{M_{O_2} P_{elec} \lambda}{4 V_c F} \quad (2)$$

Where,
$\dot{m}_{O_2}$ = oxygen mass flow rate required by the stack (kg/s)
M_{O_2} = molar mass of hydrogen (31.998g/mol [35])
P_{elec} = fuel cell electrical power request (W)
λ = stoichiometric ratio
V_c = average cell voltage (V)
F = Faraday constant (96,485C/mol [30])

Current commercial FC stacks fall into two main categories based on the cooling method used: Air-Cooled (AC) and Liquid-Cooled (LC). Generally, air cooling is used when the gross stack power is ≤5kW [36]. Due to the inherent design differences between the two cooling options, both stack designs have different gravimetric and volumetric power densities. Existing commercial stack data from Ballard, Horizon Energy Systems, Hydrogenics, Intelligent Energy and Pragma [36-46] was used to find average parameters, Table 3.

Table 3. Average power densities from commercial PEM FC stack data [36-46]

Cooling option	**Average gravimetric power density (kW/kg)**	**Average volumetric power density (kW/litre)**
AC	0.303	0.189
LC	0.443	0.540

The Department of Energy (DOE) has set targets [47] to improve the gravimetric and volumetric power densities of PEM FCs. These are summarised in Table 4.

Table 4. DOE targets for 80kW (net) integrated transportation FC power systems operating on direct hydrogen [47]

	2020 targets	**Ultimate targets**
Gravimetric power density (kW/kg)	0.65	0.85
Volumetric power density (kW/litre)	0.65	0.85

To provide a visual representation of the modelled FC to the user, data to produce polarisation and power curves was calculated. Equation 3 was used to combine the irreversible voltage losses associated with activation, ohmic resistance and mass transport within the FC of an air-breathing design [48]. Cell voltage was calculated for a range of current densities so that a polarisation curve could be generated.

$$V_c = E_{0_{HHV}} - \frac{RT}{2\alpha F} ln\left(\frac{i+i_n}{i_0}\right) - i\Omega - me^{ni} \quad (3)$$

Where,
V_c = average cell voltage (V)
$E_{0_{HHV}}$ = thermodynamic reversible voltage based on the higher heating value (HHV) of hydrogen (1.23V [33, 48-50])
R = universal gas constant (8.314J/molK [30])
T = operating temperature (323.15K, low temperature chosen to improve efficiency [50])
α = charge transfer coefficient (0.5 [48, 49])
F = Faraday constant (96,485C/mol [30])
i = current density (A/cm^2)
i_n = internal and fuel crossover equivalent current density (0.002A/cm^2 [33, 50])
i_0 = exchange current density (3.0x10^{-6}A/cm^2 [50])
Ω = ohmic resistance (0.245Ωcm^2 [49])
m = mass transport loss empirical constant 1 (3.0x10^{-5}V [49])
n = mass transport loss empirical constant 2 (7cm^2/A similar to [49])

The relationship between reactant partial pressures and FC performance is described by the Nernst equation [33, 48-50] shown in Equation 4. If the FC is supplied with pure O_2 instead of air, the performance will improve as the partial pressure of O_2 will increase.

$$V_c = E_{0_{HHV}} + \frac{RT}{2F}\ln\left(\frac{P_{H_2}.P_{O_2}^{\frac{1}{2}}}{P_{H_2O}}\right) \quad (4)$$

Where,
V_c = average cell voltage (V)
$E_{0_{HHV}}$ = thermodynamic reversible voltage based on the HHV of hydrogen (1.23V [33, 48-50])
R = universal gas constant (8.314J/molK [30])
T = operating temperature (323.15K, low temperature chosen to improve efficiency [50])
F = Faraday constant (96,485C/mol [30])
P_{H_2} = partial pressure of hydrogen (Pa)
P_{O_2} = partial pressure of oxygen (Pa)
P_{H_2O} = partial pressure of water in exhaust (Pa)

Given that the molar proportion of air that is O_2 is 0.21 [48], the change in cell voltage expected by using pure O_2 instead of air is given by Equation 5 [50].

$$\Delta V_c = \frac{RT}{2F}\ln\left[\left(\frac{1}{0.21}\right)^{0.5}\right] + \frac{RT}{\alpha F}\ln\left(\frac{1}{0.21}\right) \quad (5)$$

Where,
V_c = average cell voltage (V)
$E_{0_{HHV}}$ = thermodynamic reversible voltage based on the HHV of hydrogen (1.23V [33, 48-50])
R = universal gas constant (8.314J/molK [30])
T = operating temperature (323.15K, low temperature chosen to improve efficiency [50])
F = Faraday constant (96,485C/mol [30])
α = charge transfer coefficient (0.5 [48, 49])

Using the operating conditions shown above, the change in cell voltage expected by using pure O2 was calculated to be,

$$\Delta V_c = 0.0152V$$

By defining the desired FC operating point as a target power of 250W and an operating cell voltage of 0.6V the number of cells in the FC was calculated for both an air breathing and air independent design. These were found to be 42 cells for the air breathing system and 41 cells for the air independent system. Polarisation and power curves were then generated and collated in Figure 2.

Increased performance is represented by the higher average cell voltage on the polarisation curve and higher potential peak power. In addition to the thermodynamic effect of using pure O_2 demonstrated by Equation 5, operation with pure O_2 usually eliminates the mass transport polarisation also shown in Figure 2.

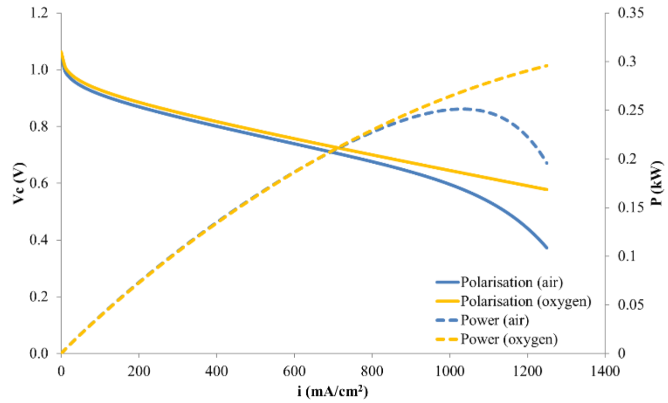

Figure 2. Modelled polarisation and power curves based on desired operating point for air breathing and air independent FC designs

Balance of Plant Model

In addition to the stack, the other key components in a FC system are collectively referred to as the Balance of Plant (BoP). The cooling and fuelling subsystems are the most significant components of the BoP in terms of mass and volume. Both will need to be considered when calculating the total mass and volume of the FC system.

Cooling

Balance of plant components required for Air-Cooled (AC) fuel cells are substantially different to those required for Liquid-Cooled (LC) fuel cells.

For this cooling method, generally a fan is used to provide airflow which is directed across the cells by some form of cowling. To calculate the mass of this subsystem, both the mass of the fan and the cowling must be found. The actual mass of fan required for the desired airflow was found from a relationship derived from commercial fans [51-53].

The volume of the subsystem was found by combining the estimated dimensions of the FC stack with the depth of the subsystem. Fan depth found from a relationship derived from commercial data [51-53].

Commercial LC fuel cells are generally accompanied by cooling module designed in-house. A typical LC subsystem may include: working liquid, liquid container, pumps, radiator and a cooling fan. Scaling factors were based on the ratio of FC stack mass and volume to cooling subsystem mass and volume of Ballard FCveloCity-HD systems [45]. These are summarised in Table 5.

Table 5. Liquid-cooling subsystem scaling factors [46]

LC subsystem mass	17% of stack mass
LC subsystem volume	29% of stack volume

The Department of Energy (DOE) has set target of reducing the mass of the air delivery and humidification systems by 23% by 2020 [47].

Fuel Storage and Delivery

Both the fuel, generally H_2 and an oxidant, generally O_2 must be delivered to the FC continuously during flight. The fuel and oxidant can either be stored on-board the aircraft or generated by breaking down water through electrolysis. An electrolyser will require its own power source which will add to the complexity of the system. To avoid this complexity, and the keep the system as light as possible both fuel and oxidant will be stored on the aircraft. Details of how the storage and delivery model was made are given separately for the fuel and oxidant.

Hydrogen

Hydrogen fuel must be stored on-board the aircraft in a sufficient quantity to meet the desired endurance requirement. In addition, the mass, volume and ease of refuelling are all critical parameters of the fuelling system. Figure 3 shows the gravimetric and volumetric storage densities of various hydrogen storage options. As aerospace applications tend to be more mass sensitive than volume sensitive, metal hydride H_2 storage would be the least suitable solution. Ideally, light hydrides would be used, however, they are generally more difficult to re-fuel due to their availability. This leaves Liquid H_2 (LH_2) and high pressure Compressed Gaseous H_2 (CGH_2) as remaining storage options.

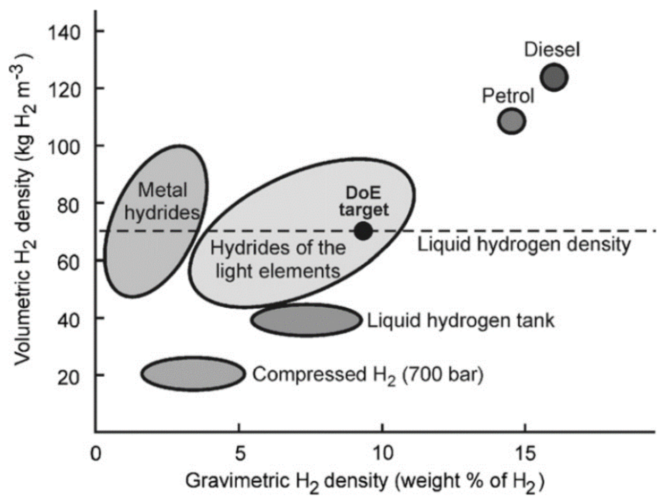

Figure 3. Gravimetric and volumetric densities of various hydrogen storage options. 'DoE target' represents the US Department of Energy target for hydrogen storage material [54].

Although widely available, both CGH_2 and LH_2 have their inherent disadvantages. For CGH_2, the high storage pressures of up to 700bar [55] required to improve storage efficiencies may not gain public acceptance due to the perceived risk [56]. Whereas, for LH_2 the key issue surrounds a phenomenon called 'boil-off' [56-57]. This is caused by the temperature of the gas increasing above its boiling point, for H_2 this is 20.3K. The evolved gas is then released to the atmosphere to avoid over pressurisation.

High pressure CGH_2 is gaining acceptance in the automotive industry, leading to an increase in compatible fuelling infrastructure. To tap in to this growing resource, it would be desirable to use CGH_2 in aviation. However, the low storage efficiency compared to LH_2 may limit use to smaller short-range aircraft. Commercial data [58-62] was used to find a cut-off point between the two storage options by relating the mass of H_2 stored to the total mass and volume of the storage system. The results are shown in Figure 4.

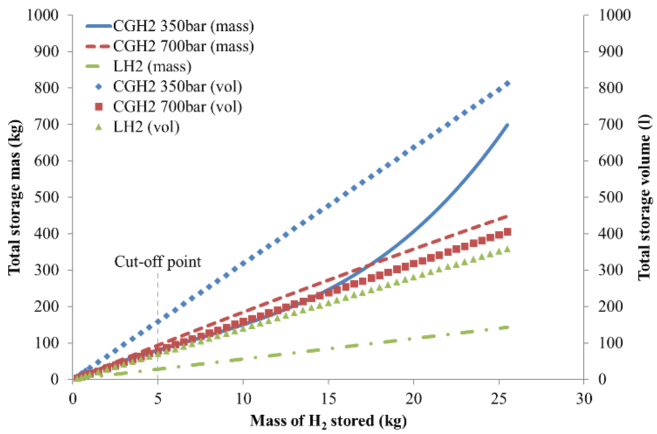

Figure 4. Total H_2 storage system mass and volume change with respect to mass of H_2 stored with preferred use cut-off point shown

Based on the total mass of the storage system, 350bar CGH_2, 700bar CGH_2 and LH_2 all show similar performance up to 5kg of H_2 stored. Above this point, both CGH_2 options diverge and increase faster than the LH_2 storage solution.

Based on the total volume occupied by the storage system, 700bar CGH_2 and LH_2 show similar performance up to 5kg of H_2 stored whereas, the 350bar CGH_2 solution occupies a significantly larger volume. Above 5kg of H_2 stored, the LH_2 system always occupies a smaller volume than 700bar CGH_2.

Combining these two relationships gives a cut-off point of 5kg of H_2 stored. For quantities of H_2 less than 5kg, 700bar CGH_2 should be used due to the larger volume occupied by 350bar CGH_2. Above this point LH2 should be used due to the significantly higher mass of the CGH_2 solutions.

Oxidant

Oxidant, generally O_2 can either be extracted from the ambient air in an air breathing system, or stored on-board in pure form in an air independent system. The main aircraft specific consideration for which system should be used is flight altitude. To investigate the effect of increasing altitude on the operation of an air breathing FC system, the power required to compress the necessary inlet air was calculated over a range of altitudes. The power of a FC suitable compressor can be found from Equation 6 [49].

$$P_{comp} = c_p \frac{T_1}{\eta_c}\left(\left(\frac{P_2}{P_1}\right)^{\frac{\gamma-1}{\gamma}} - 1\right)\dot{m} \quad (6)$$

Where,
P_{comp} = compressor power (W)
c_p = specific heat capacity of air (1004J/kgK [49])
T_1 = compressor inlet temperature (K)
η_c = isentropic compressor efficiency (0.7 used as a typical value [49])
P_2 = compressor exit pressure (FC inlet pressure) (2.0bar [49])
P_1 = compressor inlet pressure (bar)
γ = ratio of specific heat capacities of air (1.4 [49])
$\dot{m}$ = required air mass flow (kg/s)

The fuel cell model was used to calculate the required air mass flow based on the parameters in Table 6. This was found to be 0.02kg/s.

Table 6. Parameters used to find air mass flow for compressor power variation with altitude investigation

Parameter	Value
FC power	15kW
Cathode stoichiometry	2
Number of cells	500
Operating current	50A

Air pressure and temperature both vary with altitude [63]. Data from the International Standard Atmosphere (ISA) [63] was used to calculate the compressor power requirement for a range of altitudes. The results are shown in Figure 5.

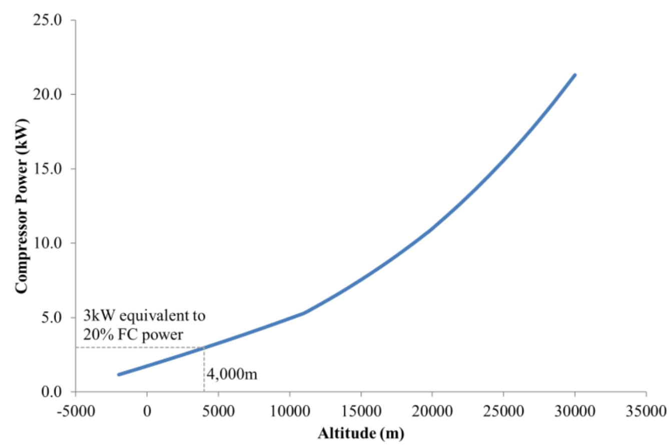

Figure 5. Air density variation with altitude between 5,000m below sea-level to 30,000m above sea-level [64]

At an altitude of 4,000m (≈13,000ft) the power required by the compressor to meet the inlet air mass flow requirement was 20% of that produced by the FC. This is an excessive parasitic load for an aircraft fuel cell therefore, an air independent system will be required for any aircraft operating at an altitude above 4,000m. An air breathing design will be used for altitudes less than 4,000m.

The main component of an air independent system is a method of storing pure O_2 on-board the aircraft in a sufficient quantity to meet the desired endurance and cooling requirements. The same methodology was used to find the most suitable O_2 storage method as was used for H_2 storage using commercial data [58-62, 64-66]. The results are shown in Figure 6.

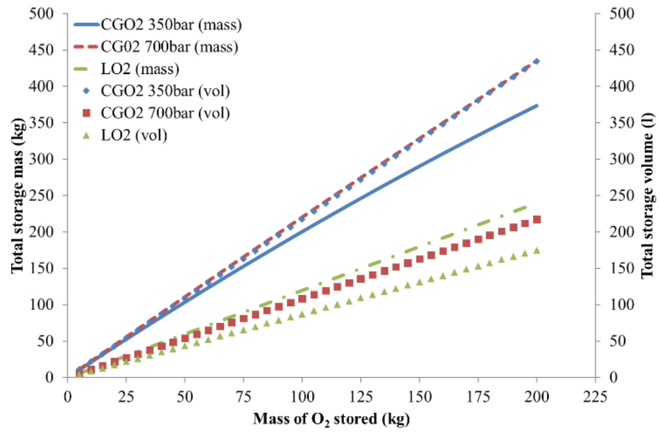

Figure 6. Total O_2 storage system mass and volume change with respect to mass of O_2 stored

Based on the total mass and volume of the storage systems, LO_2 is the only storage solution which shows good performance. Liquid oxygen storage will be used on all aircraft flying at an altitude over 4,000m.

Combined Model

Combined fuel cell sizing model is a combination of the aircraft categorisation, fuel cell sizing and balance of plant models detailed previously. The user is given the option of bypassing the aircraft categorisation model if the electrical requirements are known.

The aim of the combined model is to combine user inputs with the previously defined calculations to provide high-level FC data as well as the overall mass and volume of the FC system.

Figure 7 shows the process flow of the combined model. User inputs are shown along with interconnects between the sub-models.

Results and discussion

Aircraft Categorisation Validation

Outputs from the aircraft categorisation model were compared with real data for a selection of production aircraft. A range of categories were used for validation as each is based on different relationships. Validation results are shown in Table 7.

The results from the validation show a good correlation between the real and modelled data. Generally, an error of less than 5% was obtained by the model. Certain instances were higher than this cut-off. This occurs in cases where a category consists of a small data set.

Figure 7. Model process flow

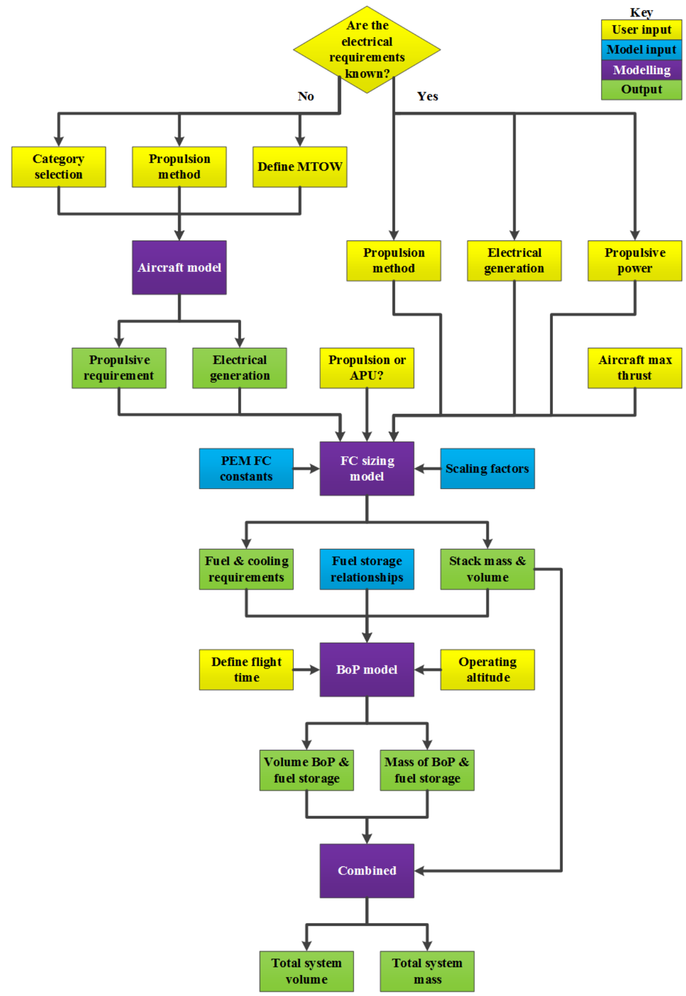

Table 7. Aircraft categorisation model validation

Aircraft	**Propulsive power / max thrust**			**Electrical generation capability**		
	Real	Model	Error	Real	Model	Error
DLR HY4	80kW	80kW	0%	45kW	45kW	0%
Airbus C212	1,380kW	1,286kW	7%	18kW	19kW	5%
Lockheed Martin F-35B	191kN	197kN	3%	60kW	60kW	0%
Airbus A400M	38,776kW	37,989 kW	2%	225kW	225kW	0%
Airbus A330-200	632kN	643kN	2%	259kW	277kW	7%
Reims F406	746kW	728kW	2%	7kW	8kW	11%
Cirrus SR22	231kW	234kW	1%	2kW	2kW	0%

Given the wide range of aircraft types catered for by the model and its function to provide a guide to manufacturers, a 10% error in the aircraft categorisation model was deemed acceptable. This error will be improved by modifying the relationships with data from more aircraft when it is available.

Overall, the aircraft categorisation model can accurately predict the electrical generation capability and propulsive requirements across the 15 defined aircraft categories.

Combined Model Results

Results for the combined model were highlighted using two wildly different aircraft as examples. The first example is a small lightweight UAV designed to use a FC as the primary power source for propulsion. This style of aircraft is designed for low altitude operation and could either be autonomous or remotely piloted from the ground. Full input parameters and model outputs are consolidated in Table 8.

Table 8. Input selections and model outputs for a typical small FC powered UAV

Input		Output		
Aircraft category	Fuel cell	FC power		250W
Propulsion method	Propeller	Number of cells		42
FC for propulsion or APU?	Propulsive power	Cooling option		Air
MTOW	7kg	Cathode inlet		Ambient
Endurance	5hrs	Mass	FC stack	0.83kg
			Fuel including storage	2.20kg
			BoP	0.44kg
Operating altitude	100m	Volume	FC stack	1.33litres
			Fuel including storage	1.87litres
			BoP	0.06litres

The results for the small FC powered UAV example show that the model correctly predicted an air breathing design based on the low operating altitude of 100m. Key high-level FC data is also provided in the form of total FC power and the number of cells required in the stack. The total system mass, including all fuel is less than 50% of the MTOW and provides up to a five-hour flight time.

The total electrical energy used by this system is 1,250Wh if it is assumed the FC operates at maximum power for the full five hours. A similar capacity battery can be made by using four cells from the 2016 Nissan Leaf, this would have a mass of 8.5kg [67]. This represents a 59% mass saving by using the FC system instead of the battery.

A large civil airliner was used as the second example. In this case, the FC would be used as an APU and required to operate over a short-haul flight time of six hours. The model input parameters are based on an Airbus A320 [19-21, 24], these are shown in Table 9 along with the model outputs.

Table 9. Input selections and model outputs for an airbus A320

Input		Output		
Aircraft category	Airliner and freighter	FC power		162kW
Propulsion method	Jet	Number of cells		2694
FC for propulsion or APU?	APU	Cooling method		Liquid
MTOW	73,500kg	Cathode inlet		On-board O_2
Endurance	6hrs	Mass	FC stack	364.4kg
			Fuel including storage	1,828kg
			BoP	244.8kg
Operating altitude	12,130m	Volume	FC stack	299.3litres
			Fuel including storage	1,918litres
			BoP	128.6litres

An air independent design is correctly produced by the model as a result of the 12,130m operating altitude. The model gives a total FC system mass of ≈2,500kg including the LC FC stack, on-board H_2 and O_2 storage and associated BoP. This is more than double the mass of an existing Honeywell 131-9[A] APU which weighs 944kg, including the fuel burnt during six hours of continuous operation assuming an operating efficiency of 25% [68].

The large mass difference between the FC system and existing system is largely a result of the inefficient storage solutions available for hydrogen and oxygen. A possible alternative would be to use SOFC technology as it is capable of being fuelled by light hydrocarbons which could potentially be stored in a similar manner to current jet fuel. The use of SOFCs in aircraft has been a topic of extensive research [4, 69-70] with key conclusions meriting the efficiency of SOFC technology and the potential to use the high-quality waste heat.

Even though current PEM FC technology cannot be used to completely replace the APU on large civil airliners, partial substitution of existing electrical generation equipment for fuel cell technology should be considered on a case-by-case basis [14].

Conclusions

Fifteen aircraft categories have been defined based on the aircrafts primary function and propulsion method. A model was then developed which can predict the electrical generation capability and propulsive requirements. Validating the categorisation model against real aircraft data showed a good correlation between the real and modelled data. Generally, an error of less than 5% was obtained by the model. Certain instances, higher than this cut-off percentage arose when the model was based off a small dataset.

An investigation was carried out into the most suitable storage method for both hydrogen and oxygen as both will be required for certain fuel cell system designs. It was found that if the amount of hydrogen required is less than five kilograms then it should be stored as a compressed gas at 700bar. For amounts of hydrogen above five kilograms, liquid storage should be used. Oxygen should always be stored in liquefied form as it is the most efficient method by both mass and volume.

The fuel cell model was based on current polymer electrolyte membrane technology and can appropriately define key, high-level parameters. By considering the ambient conditions and altitude a congruous cathode fuelling option. This lead to either an air breathing or air independent system design.

Total fuel cell system mass and volume are calculated by the combined model. These could be used by aircraft manufacturers, both military and small civil as a guide in the detailed design phase. For larger aircraft, it was found that current polymer electrolyte membrane fuel cell technology is not able to match the gravimetric power density of existing auxiliary power units. However, partial substitution of existing electrical generation equipment for fuel cell technology should be considered on a case-by-case basis.

References

1. IATA, "IATA 2015 Report on Alternative Fuels," http://www.iata.org/publications/Documents/2015-report-alternative-fuels.pdf, accessed Mar. 2017.
2. Wang, Y., Chen, K., Mishler, J., Cho, S C. et al., "A Review of Polymer Electrolyte Membrane Fuel Cells: Technology, Applications, and Needs on Fundamental Research," *Applied Energy* 88(4):981-1007, 2011, doi:10.1016/j.apenergy.2010.09.030.
3. Kumar, L. and Jain, S., "Electric Propulsion System for Electric Vehicular Technology: A Review," *Renewable and Sustainable Energy Reviews* 29(01):924-940, 2014, doi:10.1016/j.rser.2013.09.014.
4. Aguiar, P., Brett, D. and Brandon, N., "Solid Oxide Fuel Cell/Gas Turbine Hybrid System Analysis for High-altitude Long-endurance Aerial Vehicles," *International Journal of Hydrogen Energy* 33(23):7214-7223, 2008, doi:10.1016/j.ijhydene.2008.09.012.
5. Bradley, T., Moffit, B., Marvis, D. and Parekh, D., "Development and Experimental Characterisation of a Fuel Cell Powered Aircraft," *Journal of Power Sources* 171(2):793-801, 2007, doi:10.1016/j.jpowsour.2007.06.215.
6. Dudek, M., Tomczyk, P., Wygonik, P., Korkosz, M. et al., "Hybrid Fuel Cell – Battery System as a Main Power Unit for Small Unmanned Aerial Vehicles (UAV)," *International Journal of Electrochemical Science* 8(6):8442-8463, 2013.
7. Renouard-Vallet, G., Kallo, D., Friedrich, A., Schirmer, J. et al., "Fuel Cells for Aircraft Applications," *ECS Transactions* 30(1):271-280, 2011, doi:10.1149/1.3562482.
8. Guynn, M., Freh, J. and Olson, E., "Evaluation of a Hydrogen Fuel Cell Powered Blended-wing-body Aircraft Concept for Reduced Noise and Emissions," https://ntrs.nasa.gov/archive/nasa/casi.ntrs.nasa.gov/20040033924.pdf, accessed Nov. 2016.
9. Herwerth, C., Chiang, C., Ko, A., Matsuyama, S. et al., "Development of a Small Long Endurance Hybrid PEM Fuel Cell Powered UAV," SAE Technical Paper 2007-01-3930, 2007, doi:10.4271/2007-01-3930.
10. Kim, K., Kim, T., Lee, K. and Kwon, S., "Fuel Cell System with Sodium Borohydride as Hydrogen Source for Unmanned Aerial Vehicles," *Journal of Power Sources* 196(21):9069-9075, 2011, doi:10.1016/j.jpowsour.2011.01.038.
11. Kim, T. and Kwon, S., "Design and Development of a Fuel Cell-Powered Small Unmanned Aircraft," *International Journal of Hydrogen Energy* 37(1):615-622, 2012, doi:10.1016/j.ijhydene.2011.09.051.
12. Lapeña-Rey, N., Mosquera, J., Bataller, E., Ortí, A. et al., "Environmentally Friendly Power Sources for Aerospace Applications," *Journal of Power Sources* 181(2):353-362, 2008, doi:10.1016/j.jpowsour.2007.11.045.
13. McConnell, V., "Military UAVs Claiming the Skies with Fuel Cell Power," Fuel Cells Bulletin: 12-15, Dec. 2007.
14. Pratt, J., Klebanoff, L., Munoz-Ramos, K., Akhil, A. et al., "Proton exchange Membrane Fuel Cells for Electrical Power Generation On-Board Commercial Airplanes," *Applied Energy* 101(1):776-796, 2013, doi:10.1016/j.apenergy.2012.08.003.
15. Pratt, J., Brouwer, J. and Samuelsen, G., "Performance of Proton Exchange Membrane Fuel Cell at High-Altitude Conditions," *Journal of Propulsion and Power* 23(2):437-444, 2012, doi:10.2514/1.20535.
16. Renau, J., Lozano, A., Barroso, J., Miralles, J. et al., "Use of Fuel Cell Stacks to Achieve High Altitudes in Light Unmanned Aerial Vehicles," *International Journal of Hydrogen energy* 40(42):14573-14583, 2015, doi:10.1016/j.ijhydene.2015.02.071.
17. Roth, B. and Giffin, R., "Fuel Cell Hybrid Propulsion Challenges and Opportunities for Commercial Aviation," presented at 46th AIAA/ASME/SAE/ASEE Joint Propulsion Conference & Exhibit, USA, July 25-28, 2010.
18. Ward, T. and Jenal, N., "Design and Initial Flight tests of a Hydrogen Fuel Cell Powered Unmanned Air Vehicle (UAV)," *ECS Transactions* 26(1):433-444, 2010, doi:10.1149/1.3429016.
19. Jackson, P., Gunston, B., Willis, D., Munson, K. et al., "Jane's All the World's Aircraft: Development & Production 2014-2015," (IHS, 2014), ISBN:978-0710630933.
20. Jackson, P., Gunston, B., Willis, D., Munson, K. et al., "Jane's All the World's Aircraft: Development & Production 2015-2016," (IHS, 2015), ISBN:978-0710631359.
21. Jackson, P., Gunston, B., Willis, D., Munson, K. et al., "Jane's All the World's Aircraft: Development & Production 2016-2017," (IHS, 2016), ISBN:978-0710631770.
22. Endres, G., Gething, M., "Jane's Aircraft Recognition Guide," (Collins, 2007), ISBN:978-0007257928.
23. Streetly, M., "Jane's All the World's Aircraft: Unmanned 2015-2016," (IHS, 2015), ISBN:978-07106313381.
24. Airbus Training, "A320-Electrical," http://www.smartcockpit.com/docs/A320-Electrical.pdf, accessed Mar. 2017.
25. Airbus Training, "A330-Electrical," http://www.smartcockpit.com/docs/A330-Electrical.pdf, accessed Mar. 2017.

26. Airbus Training, “A340-Electrical,” http://www.smartcockpit.com/docs/FCOM_A340-Electrical.pdf, accessed Mar. 2017.
27. General Atomics – Aeronautical Systems Inc., “MQ-9 Reaper/Predator,” http://www.ga-asi.com/Websites/gaasi/images/products/aircraft_systems/pdf/MQ9%20Reaper_Predator_B_032515.pdf, accessed Mar. 2017.
28. General Atomics – Aeronautical Systems Inc., “Predator B,” http://www.ga-asi.com/Websites/gaasi/images/products/aircraft_systems/pdf/Predator_B021915.pdf, accessed Mar. 2017.
29. Boeing, “F-15 Strike eagle,” http://www.boeing.com/defense/f-15-strike-eagle/, accessed Mar. 2017.
30. Tavares, S., “Aerospace Engineering Pocket reference,” (Taylor & Francis, 2015), 278-279, ISBN:978-1498703642.
31. Middleton, M., “Better Exponential Curve Fitting Using Excel,” presented at Decision Sciences Institute Annual Meeting 41st, USA, November 20-23, 2010.
32. Microsoft, “LINEST function,” https://support.office.com/en-us/article/LINEST-function-84d7d0d9-6e50-4101-977a-fa7abf772b6d?NS=EXCEL&Version=16&SysLcid=1033&UiLcid=1033&AppVer=ZXL160&HelpId=xlmain11.chm60097&ui=en-US&rs=en-US&ad=US, accessed Mar. 2017.
33. Larmine, J. and Dicks, A., “Fuel Cell Systems Explained, First Edition,” (John Wiley & Sons, 2000), ISBN978-0471490261.
34. PubChem Open Chemistry Database, “Hydrogen,” https://pubchem.ncbi.nlm.nih.gov/compound/Hydrogen, accessed Mar. 2017.
35. PubChem Open Chemistry Database, “Oxygen,” https://pubchem.ncbi.nlm.nih.gov/compound/977#section=Top, accessed Mar. 2017.Horizon Fuel Cell Technologies, “H-Series Stacks 10W-5kW,” http://www.horizonfuelcell.com/h-series-stacks, accessed Aug. 2016.
36. Horizon Fuel Cell Technologies, “H-500XP Designed for Efficiency,” http://media.wix.com/ugd/047f54_6ceaa64103e944008c48ae2fa33a655e.pdf, accessed Aug. 2016.
37. Horizon fuel Cell Technologies, “H-1000XP designed for Efficiency,” http://media.wix.com/ugd/047f54_d140778984ed4c61a0c5d2fc8b9df2ab.pdf, accessed Aug. 2016.
38. Horizon Energy Systems, “AEROSTACKS, World’s Lightest Fuel Cells for Electric UAVs,” https://media.wix.com/ugd/047f54_8483372175ef4e1aa43edbe62aaae68e.pdf, accessed Aug. 2016.
39. Hydrogenics, “HyPM-HD Power Modules,” http://www.hydrogenics.com/wp-content/uploads/HyPM-HD-Brochure.pdf, accessed Aug. 2016.
40. Hydrogenics, HyPM-XR Power Modules,” http://www.hydrogenics.com/wp-content/uploads/HyPM-XR-Brochure.pdf, accessed Aug. 2016.
41. Intelligent Energy Ltd., “Data Sheet, AC10 Stack,” http://www.intelligent-energy.com/uploads/accompanying_files/41556_IE_-_AC10_datasheet_no_crops.pdf, accessed Dec. 2016.
42. Intelligent energy Ltd., “Data Sheet, AC64 Stack,” http://www.intelligent-energy.com/uploads/uploads/Datasheets/41556_ie_-_ac64_datasheet.pdf, accessed Dec. 2016.
43. Ballard Power systems Inc., “FCgen-1020ACS,” http://ballard.com/files/PDF/Backup_Power/1020ACS_v2.pdf, accessed Aug. 2016.
44. Ballard Power Systems Inc., “FCvelocity-9SSL,” http://ballard.com/files/PDF/Material_Handling/9SSL.pdf, accessed Aug. 2016.

45. Ballard Power Systems Inc., “FCveloCity-HD,” http://ballard.com/files/PDF/Bus/FCvelocity_HD_Family_of_Products_Low_Res.pdf, accessed Aug. 2016.
46. Pragma Industries, “Fuel Cell Systems for Projects and research Work,” http://www.pragma-industries.com/wp-content/themes/default/images/pdf_products/Brochure_FC_SYSTEMS_ENG.pdf, accessed Aug. 2016.
47. DOE., “Fuel Cell Technologies Office Multi-Year Research, Development, and Demonstration Plan - Fuel Cells,” https://energy.gov/sites/prod/files/2016/10/f33/fcto_myrdd_fuel_cells.pdf, accessed Mar. 2017.
48. O’Hayre, R., Cha, S., Colella, W. and Prinz, F., “Fuel Cell Fundamentals, Third Edition,” (John Wiley & Sons, 2016), ISBN:978-1119113805.
49. Larmine, J. and Dicks, A., “Fuel Cell Systems Explained, Second Edition,” (John Wiley & Sons, 2003), ISBN:978-0470848579.
50. Barbir, F., “PEM Fuel Cells Theory and Practice,” (Elsevier Academic Press, 2005), ISBN:978-0080455419.
51. Sunon, “DR Maglev DC Brushless Fan & Blower,” http://docs-europe.electrocomponents.com/webdocs/10f0/0900766b810f0b52.pdf, accessed Mar. 2017.
52. ebmpapst, “Automotive brushless DC fans Climate control for commercial vehicles Automotive brushless DC fans,” http://docs-europe.electrocomponents.com/webdocs/140a/0900766b8140a813.pdf, accessed Mar. 2017.
53. ebmpapst, “W4E400A Series,” http://docs-europe.electrocomponents.com/webdocs/140a/0900766b8140a82a.pdf, accessed Mar. 2017.
54. Edwards, P., Kuznetsov, V., David, W. and Brandon, N., “Hydrogen and Fuel cells: Towards a Sustainable Energy Future,” *Energy Policy* 36(12):4356-4362, 2008, doi:10.1016/j.enpol.2008.09.036.
55. Gray, E., “Hydrogen Storage – Status and Prospects,” *Advances in Applied Ceramics* 106(1):25-28, 2007, doi:10.1179/174367607X152380.
56. Schlapbach, L. and Züttel, A., “Hydrogen-Storage Materials for Mobile Applications,” *Nature* 414(1):353-358, 2001, doi:10.1038/35104634.
57. Hirscher, M., “Handbook of Hydrogen Storage: New Materials for Future Energy Storage,” (Wiley-VCH, 2010), doi:10.1002/9783527629800.
58. Horizon Fuel Cell Technologies, “Ultra-light Composite Cylinder (E-Series),” http://www.fuelcellstore.com/hydrogen-equipment/hydrogen-storage/composite-storage-cylinders/ultra-light-composite-storage-cylinder-e-series, accessed Jan. 2017.
59. Luxfer Gas Cylinders, “G-Stor™ H2 Hydrogen-Storage Cylinders,” http://www.luxfercylinders.com/products/alternative-fuel/gstorh2, accessed Jan. 2017.
60. Mahytec, “Hydrogen Storage Solutions,” http://www.mahytec.com/en/our-solutions/, accessed Jan. 2017.
61. Steelhead Composites, “Hydrogen Gas Storage,” http://steelheadcomposites.com/products/gas-cylinders/hydrogen/, accessed Jan. 2017.
62. Lapesa, “Horizontal Cryogenic Tanks,” www.lapesa.es/descargar.php?f=/sites/default/files/documentos/gnli_1011.pdf, accessed Jan. 2017.
63. Cavcar., “The International Standard Atmosphere (ISA),” *Anadolu University, Turkey* 1-7, ISBN:92-9194-004-6.
64. Quantum Fuel Systems, “Q-Lite™ Advanced CNG Fuel Storage Tanks,” http://www.qtww.com/product/q-lite-lightest-cng-tanks/, accessed Jan. 2017.

65. Luxfer Gas Cylinders, "L6X Composite Inflation and Aerospace Cylinders," http://www.luxfercylinders.com/products/l6x-composite-cylinder, accessed Jan. 2017.
66. Chart Industries, "CAIRE Liquid Oxygen Reservoirs," http://www.chartindustries.com/Respiratory-Healthcare/Liquid-Oxygen-Systems/Reservoirs, accessed Jan. 2017.
67. EV Battery Center, "Lithium Battery Module LiMn2O4/LiNiO2," http://evbatterycenter.com/HAC4/index.php?option=com_hikashop&ctrl=product&task=show&cid=211&name=82ah-nissan-leaf-battery-module-500wh-4x-cells-82ah&Itemid=686, accessed Mar. 2017.
68. Honeywell, "APU 131-9(A)," http://www51.honeywell.com/aero/common/documents/myaerospacecatalog-documents/ATR_Brochures-documents/131-9A_US.pdf, accessed Mar. 2017.
69. Himansu, A., Freeh, J., Steffen, C., Tornabene, A. et al., "Hybrid Solid Oxide Fuel Cell / Gas Turbine System Design for High Altitude Long Endurance Aerospace Missions," presented at 4th International ASME Conference on Fuel Cell Science, Engineering and Technology, USA, June 19-21, 2006.
70. NASA, "Emerging Fuel Cell Developments at NASA for Aircraft Applications," https://www.netl.doe.gov/File%20Library/Events/2003/seca/Anita-Liang.pdf, accessed Mar. 2017.

Nomenclature

c_p	specific heat capacity of air (1004J/kgK)
$E_{0_{HHV}}$	thermodynamic reversible voltage based on the higher heating value (HHV) of hydrogen (1.23V)
F	Faraday constant (96,485C/mol)
H_2	hydrogen
i	current density (A/cm^2)
i_0	exchange current density (A/cm^2)
i_n	internal and fuel crossover equivalent current density (A/cm^2)
m	mass transport loss empirical constant 1 (3.0x10^{-5}V)
$\dot{m}$	required air mass flow (kg/s)
$\dot{m}_{H_2}$	hydrogen mass flow rate required by the stack (kg/s)
$\dot{m}_{O_2}$	oxygen mass flow rate required by the stack (kg/s)
M_{H_2}	molar mass of hydrogen (2.016g/mol)
M_{O_2}	molar mass of hydrogen (31.998g/mol)
n	mass transport loss empirical constant 2 (7cm^2/A)
O_2	oxygen
P_1	compressor inlet pressure (bar)
P_2	compressor exit pressure (FC inlet pressure) (bar)
P_{comp}	compressor power (W)
P_{elec}	fuel cell electrical power request (W)
P_{H_2}	partial pressure of hydrogen (Pa)
P_{H_2O}	partial pressure of water in exhaust (Pa)
P_{O_2}	partial pressure of oxygen (Pa)
R	universal gas constant (8.314J/molK)
R^2	coefficient of determination
T	operating temperature (K)
T_1	compressor inlet temperature (K)
V_c	average cell voltage (V)

Greek characters,

α	charge transfer coefficient
γ	ratio of specific heat capacities of air (1.4)
η_c	isentropic compressor efficiency (0.7)
λ	stoichiometric ratio
Ω	ohmic resistance (Ωcm^2)

Contact Information

Professor Rui Chen
Department of Aeronautical and Automotive Engineering
Loughborough University, LE11 3TU
email: r.chen@lboro.ac.uk

Acknowledgments

Funding from EPSRC CDT in Fuel Cells and their Fuels: EP/L015749/1.

Content reviewed and agreed for public release by BAE Systems.

Author Affiliation

Alex Thirkell	Loughborough University
Rui Chen	Loughborough University
Ian Harrington	BAE Systems

Abbreviations

AC	Air-cooled
APU	Auxiliary power unit
BoP	Balance of plant
CGH$_2$	Compressed gaseous hydrogen

DOE Department of Energy

FC Fuel cell

ISA International Standard Atmosphere

LC Liquid-cooled

LH_2 Liquid hydrogen

MTOW Maximum take-off weight

OEM Original equipment manufacturer

PEM Polymer electrolyte membrane

SOFC Solid oxide fuel cell